nature cell biology

DOI: 10.1038/ncb2095

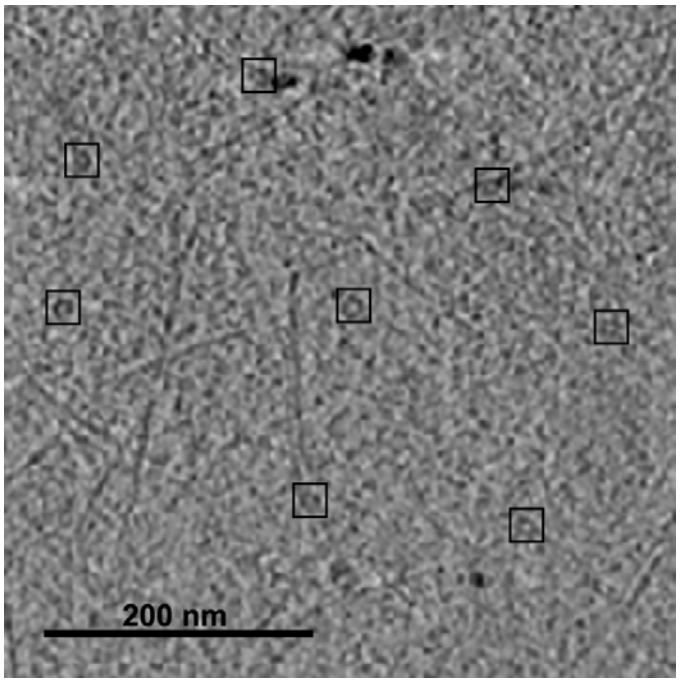

Figure S1 Adhesion-related particles at non-adhesive sites. An x-y tomographic slice, taken from the bottom of a cell, in a non-adhesive region, indicates the low density of adhesion-related particles.

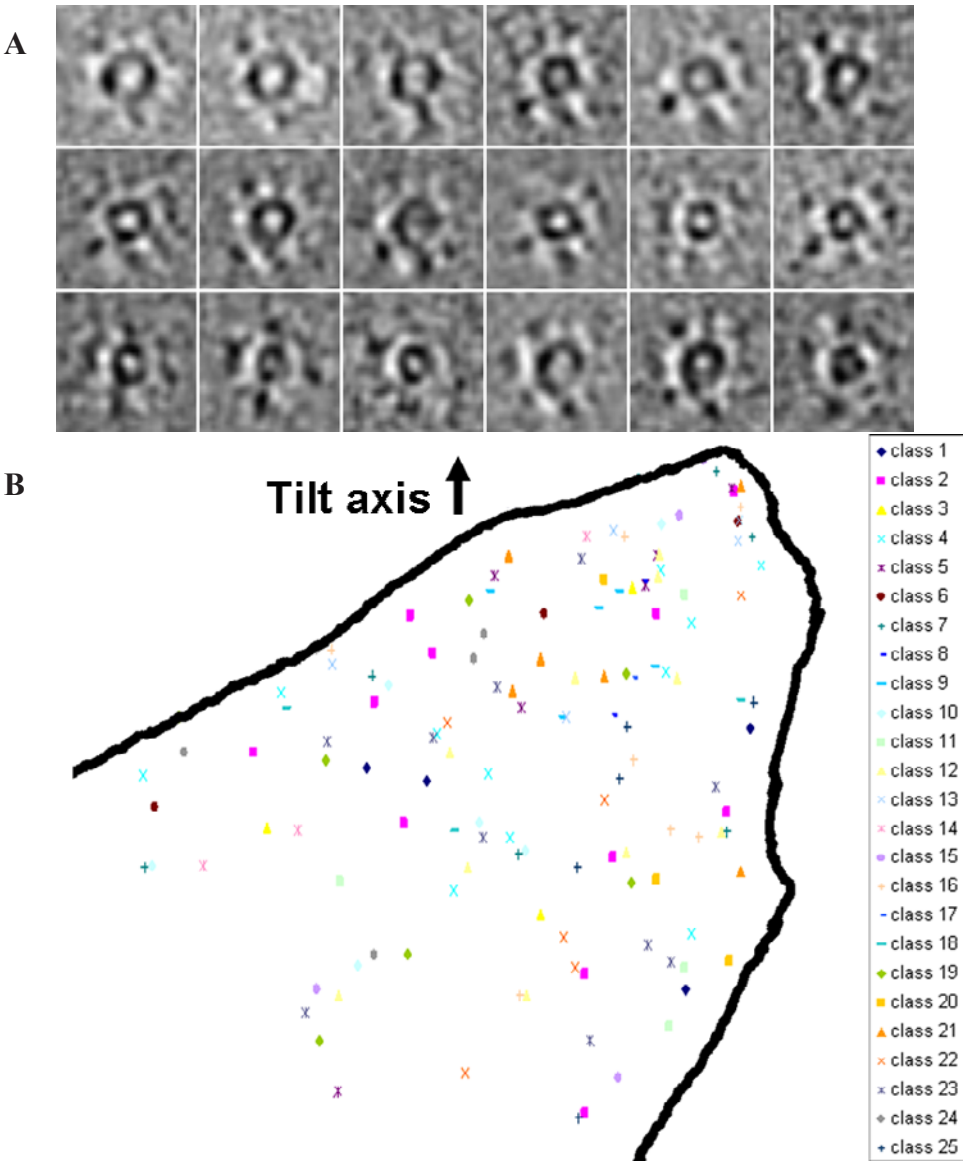

Figure S2 Class averages of the adhesion related-particles. (**A**). Of a total of 25 classes of adhesion-related particles in REF52 cells, 18 class averages are shown (see Materials and Methods). These classes were converged by iterative alignment and classification procedures. When adhesion-related particles were separated into a larger number of classes (e.g., 50 or 100), novel features were not observed, while their separation into a smaller number of classes (e.g., 10) resulted in the fading of particle features, indicating the existence of about 25 classes. It is noteworthy that the additional 7 classes not shown exhibit a small number of particles, resulting in a lower S/N ratio. (**B**) The distribution of the classes is independent of the relative position of the tilt axis, indicating the inherent structural differences among the classes.

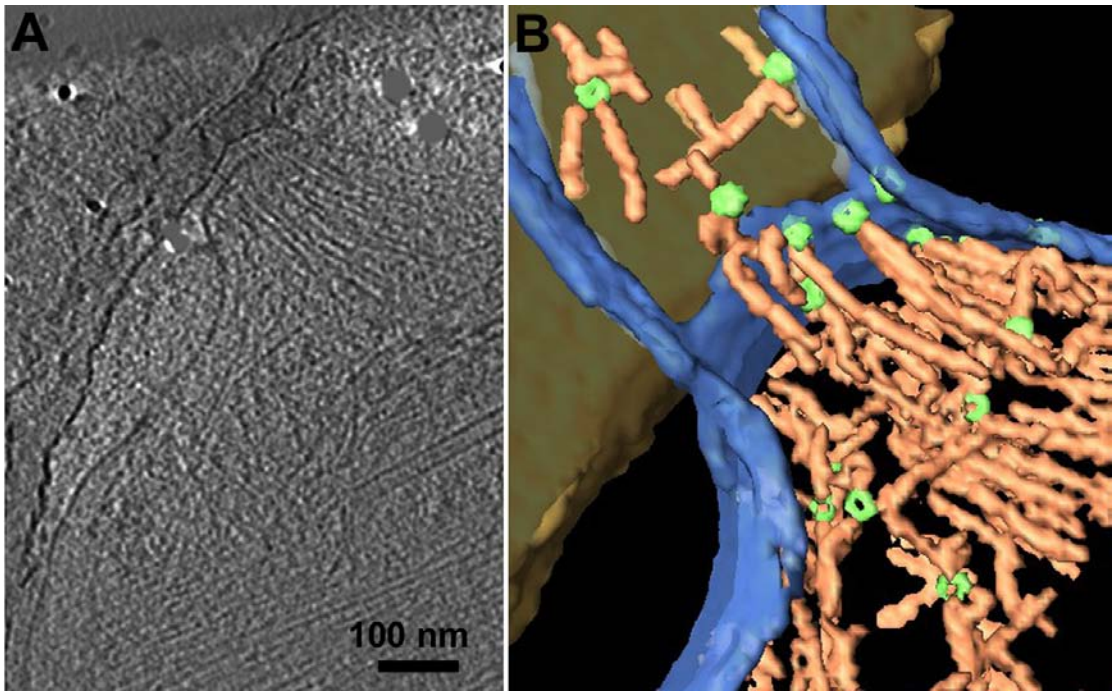

Figure S3 Adhesion-related particles are attached to the cytoplasmic aspect of the plasma membrane. (**A**) A 7-nm x-y slice through a cell that spread over a step in the carbon substrate, enabling accurate tangential visualization of the particle-plasma membrane interface. To obtain better contrast, some fiducial gold markers were masked. (**B**) Surface rendering view of the same area, displaying part of the actin network within a 480 nm × 480 nm area from the reconstructed volume shown in (**A**), indicates the close interactions of the adhesion-associated particles (light green) with the cytoplasmic aspect of the plasma membrane, bridging the cytoskeletal filaments (reddish brown) and the plasma membrane (blue).

Movie S1 Cryo-ET anlysis of focal adhesion